

Crystal chemistry aspects of the magnetically induced ferroelectricity in TbMn_2O_5 and BiMn_2O_5

This article has been downloaded from IOPscience. Please scroll down to see the full text article.

2009 J. Phys.: Condens. Matter 21 015903

(<http://iopscience.iop.org/0953-8984/21/1/015903>)

View [the table of contents for this issue](#), or go to the [journal homepage](#) for more

Download details:

IP Address: 129.252.86.83

The article was downloaded on 29/05/2010 at 16:55

Please note that [terms and conditions apply](#).

Crystal chemistry aspects of the magnetically induced ferroelectricity in TbMn_2O_5 and BiMn_2O_5

L M Volkova and D V Marinin

Institute of Chemistry, Far Eastern Branch of the Russian Academy of Sciences,
690022 Vladivostok, Russia

E-mail: volkova@ich.dvo.ru

Received 21 May 2008, in final form 30 September 2008

Published 1 December 2008

Online at stacks.iop.org/JPhysCM/21/015903

Abstract

The origin of magnetic frustration was stated and the ions, whose shift is accompanied by emerging magnetic ordering and ferroelectricity in TbMn_2O_5 and BiMn_2O_5 , were determined on the basis of calculating the magnetic coupling parameters by using the structural data. The displacements accompanying the magnetic ordering are not polar, they just induce changes of bond valence (charge disordering) of Mn1 and Mn2, thus creating instability in the crystal structure. The approximation of the bond valence to the initial value (charge ordering) under magnetic ordering conditions is only possible again due to polar displacement of Mn2 (or O1) and O4 ions along the b axis which is the cause of the ferroelectric transition.

(Some figures in this article are in colour only in the electronic version)

1. Introduction

The problem of crystal structure coupling with emerging magnetic ordering and electric polarization in multiferroics has been discussed rather intensively until recently. It was stated [1–12] that in multiferroics RMn_2O_5 (R—rare earth elements and Bi) the Mn^{3+} and Mn^{4+} ions are coupled by strong magnetic interactions competing with each other. Under applied magnetic field and at temperatures of about 40 K the antiferromagnetic ordering of Mn spins takes place, thus inducing the emerging electric polarization along the b axis. As was assumed in [6], polar atomic displacements resulted in the symmetry center disappearance and reduced the crystal symmetry from the $Pbam$ to the $Pb2_1m$ space group.

However, in spite of numerous attempts, direct experimental evidence of the presence of structural modifications accompanying the electric polarization in RMn_2O_5 has not been found yet. It must be related to the fact that until recently the structural studies of induced multiferroics RMn_2O_5 under high magnetic fields have not been conducted, since the required combination of high magnetic fields and x-ray diffraction equipment has only recently become available [13–17]. Besides, another problem in studying the multiferroics structures exists. It is concerned with the fact

that, in the process of studying different samples of the same compound RMn_2O_5 by means of x-ray powder diffraction methods, one obtains a wide range of $\text{Mn}^{3+}\text{--O}$, $\text{Mn}^{4+}\text{--O}$ and $\text{R}^{3+}\text{--O}$ bond lengths. For example, in the paraelectric phase of three samples of NdMn_2O_5 [18–20] the difference in respective $\text{Mn}^{3+}\text{--O}1$, $\text{Mn}^{3+}\text{--O}3$, $\text{Mn}^{3+}\text{--O}4$, $\text{Mn}^{4+}\text{--O}$ and $\text{Nd}\text{--O}$ bond lengths reaches 0.05, 0.06, 0.15, 0.04–0.05 and 0.04–0.13 Å, respectively. Moreover, even alternating along the c axis long and short $\text{Mn}^{4+}\text{--Mn}^{4+}$ distances and the $\text{Mn}^{3+}\text{--Mn}^{3+}$ distance in the dimer vary over too wide a range for heavy atoms: 2.93–2.99, 2.71–2.77 and 2.86–2.90 Å, respectively. On the other hand, the difference in unit cell parameters is as small as 0.02 Å. Such structural differences may result from three factors: non-stoichiometry of the NdMn_2O_5 composition, low accuracy of the measurement method used or structural instability (non-rigidity).

The emerging electric polarization at the separation of the gravity centers of positive and negative charges might be the result of the displacement of the cation itself from the polyhedron center or that of lighter oxygen anions or both types of ions. Reorientation of magnetic moments (antiferromagnetic (AF)—ferromagnetic (FM) transition) is also accompanied by displacements of intermediate ions in local space between magnetic ions. The ability of the

surrounding cations' coordination to withstand such distortions would facilitate both reorientation of magnetic moments and emergence of dipole moments. We have analyzed the crystal structures of Mn^{3+} and Mn^{4+} from the Inorganic Crystal Structure Database (ICSD) (version 1.4.4, FIZ Karlsruhe, Germany, 2008-1), which were determined with the highest accuracy by means of x-ray single-crystal diffraction (the refinement converged to the residual factor (R) values $R = 0.045\text{--}0.079$) or neutron powder diffraction ($R = 0.018\text{--}0.057$) methods. The analysis has shown that the coordination polyhedra of both Jahn–Teller ion Mn^{3+} and regular ion Mn^{4+} are not 'rigid' and meet the above requirement. The bond lengths and angles in the Mn^{3+} and Mn^{4+} polyhedra vary within a wide range in a random manner, since no regular increase of the bridge bond lengths or decrease of the end bond lengths was traced. For example, in the square pyramids $Mn^{3+}O_5$ coupled by common edges and vertices in the compounds $CaMn_2O_4$ [21], $KMnO_2$ [22], $Na_4Mn_2O_5$ [23] and $Ba_2Mn_2Si_2O_9$ [24] the lengths of the Mn^{3+} bonds with oxygen atoms located in the pyramid vertex and base vary in the ranges 2.07–2.33 and 1.70–2.25 Å, respectively. The bond valence of Mn^{3+} ions deviates significantly ($V_{Mn^{3+}} = 2.85\text{--}3.21$) from the ideal value. In the octahedra $Mn^{4+}O_6$ coupled by common edges and vertices in the compounds Pb_2MnO_4 [25], $BaMn_3O_6$ [26], $Na_2Mn_3O_7$ [27] and $Ba_4Mn_3O_{10}$ [28], the $Mn^{4+}\text{--}O$ distances and valence bonds of Mn^{4+} fall into the ranges 1.82–2.28 Å and 2.96–3.92, respectively. The ordered octahedral surrounding is observed only in high-symmetry crystals and has an enforced character.

The objective of this study is to determine which changes in the crystal structure could be the result of magnetic ordering of the frustrated antiferromagnetics $TbMn_2O_5$ and $BiMn_2O_5$ and why these changes can be the cause of emerging electrical polarization. To attain this objective, the sign and strength of magnetic interactions in the paraelectric phase of $TbMn_2O_5$ and $BiMn_2O_5$ will be calculated, and intermediate ions located in critical (or close to critical) positions of the local space between magnetic ions, deviations from which may cause reorientations of the magnetic moments and emergence of magnetic ordering, will be found. The crystal structure of the magnetically ordered phase will be determined by varying these intermediate ion coordinates, and polar ions displacements resulting in a ferroelectric transition at preserving magnetic ordering will be stated.

2. Method

The sign and strength of magnetic couplings in compounds were calculated by a new phenomenological method developed earlier [29] on the basis of structural data.

We have developed this method to estimate characteristics of magnetic interactions between magnetic ions located at any distances from each other. The main problem to be solved during the development of this method was to find a natural relation of the strength of the magnetic interactions and the type of magnetic moment ordering with crystal chemistry parameters in low-dimensional crystal compounds. For such a solution we used three widely spread concepts

of the nature of magnetic interactions, discussed below. According to Kramers [30], the exchange couplings between magnetic ions separated by one or more diamagnetic groups are characterized by a significant contribution of non-magnetic ion electrons. The crystal chemistry aspect of the model of Goodenough–Kanamori–Anderson [31] unambiguously indicates the dependence of the interaction strength and the magnetic ion spins' orientation type on the locations of intermediate ions. According to the polar model of Shubin–Vonsovsky [32], the determination of magnetic interaction characteristics should take into account not only the anions with valent bonds to magnetic ions, but also all the intermediate negatively or positively polarized atoms.

We have studied the relation of magnetic characteristics with crystal structure in low-dimensional compounds of d-elements on the experimental data provided in the literature. As a result, we have found that the interaction between magnetic ions M_i and M_j emerges in the moment of crossing the boundary of the space between them by the intermediate A_n ion. Here we take into account not only anions, which are valent-bound to the magnetic ions, but also all the intermediate negatively or positively ionized atoms, except cations of metals without unpaired electrons. The bound space region between the M_i and M_j ions along the bond line is defined as a cylinder whose radius is equal to that of these magnetic ions. If the magnetic ions are not identical, taking the radius of a smaller ion as the cylinder radius produced the best approximation to experimental results in all our cases under consideration. However, to make any final solution of this problem studies of a larger number of compounds are required. The strength of magnetic interactions and the ordering type of the magnetic moments in isolators are determined mainly by the geometrical arrangement and the size of the intermediate A_n ion in the bound space region between two magnetic ions M_i and M_j (figure 1). The distance between magnetic ions, such as inside the low-dimensional fragment and between fragments, has an effect only on the contribution value, but does not determine the sign (type) of the contribution in the case of absence of a direct interaction contribution. The value of interaction into antiferromagnetic (AF) or ferromagnetic (FM) components of the interaction is maximal, if the intermediate ion is located in the central one-third of the space between the magnetic ions. To produce the maximum contribution into the AF component the intermediate ion should be located near the axis, while for maximum contribution to the FM component, in contrast, it should be near the surface of a cylinder limiting the space area between magnetic fields.

If some intermediate ions enter the space between two magnetic ions, each of them, depending on the location, tends to orient the magnetic moments of these ions accordingly and makes a contribution to the occurrence of AF or FM components of magnetic interaction. The sign and value of the strength of the interaction J_{ij}^s between the magnetic ions M_i and M_j are determined by the sum of these contributions j_n^s :

$$J_{ij}^s = \sum_n j_n^s. \quad (1)$$

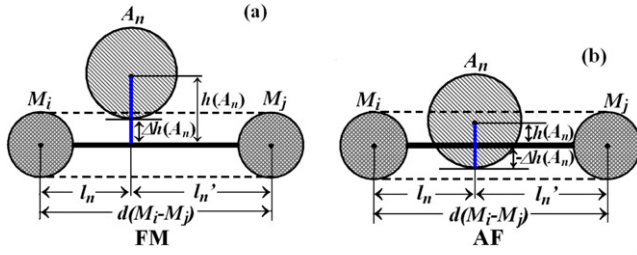


Figure 1. A schematic representation of the intermediate A_n ion arrangement in the local space between magnetic ions M_i and M_j in cases when the A_n ion initiates the emerging of the ferromagnetic (a) and antiferromagnetic (b) interactions. $\Delta h(A_n)$, l_n , l'_n and $d(M_i-M_j)$ —parameters determining the sign and strength of magnetic interactions.

If $J_{ij}^s < 0$, the type of magnetic moment ordering of M_i and M_j ions is antiferromagnetic, while if $J_{ij}^s > 0$, the type of magnetic moment ordering is ferromagnetic.

The sign and strength of the j_n^s contributions are determined by the degree of overlapping of the space between the magnetic ions by the intermediate A_n ion, the degree of asymmetry of the A_n ion location relative to the bond line M_i-M_j and the distance between magnetic fields $d(M_i-M_j)$:

$$j_n^s = \frac{\Delta h(A_n) \frac{l_n}{r_n} + \Delta h(A_n) \frac{l'_n}{r_n}}{d(M_i - M_j)^2}, \quad (\text{if } l'_n/l_n < 2), \quad (2)$$

and

$$j_n^s = \frac{\Delta h(A_n) \frac{l_n}{r_n}}{d(M_i - M_j)^2}, \quad (\text{if } l'_n/l_n \geq 2). \quad (3)$$

Here $\Delta h(A_n)$ is the difference between the distance $h(A_n)$ from the center of the A_n ion up to the bond line M_i-M_j , while r_{A_n} is the radius of the A_n ion (figure 1):

$$\Delta h(A_n) = h(A_n) - r_{A_n}. \quad (4)$$

This value characterizes the degree of space overlapping between the magnetic ions M_i and M_j . If $\Delta h(A_n) < 0$, the A_n ion overlaps (by $|\Delta h|$) the bond line M_i-M_j and initiates the emerging contribution into the AF component of magnetic interaction. If $\Delta h(A_n) > 0$, there remains a gap (the gap width Δh) between the bond line and the A_n ion, and this ion initiates a contribution to the FM component of magnetic interaction.

l_n and l'_n are the lengths of segments obtained by drawing a perpendicular from the center of the A_n ion to the bond line M_i-M_j . Let us assume that $l_n \leq l'_n$; $l'_n = d(M_i-M_j) - l_n$. The l'_n/l_n ratio characterizes the degree of asymmetry of the A_n ion location relative to the middle of the M_i-M_j straight line. If $l'_n/l_n < 2.0$, the magnetic moments of both M_i and M_j ions will be under the orientation effect of the intermediate A_n ion and the j_n^s calculation will have to be performed in accordance with formula (2). If $l'_n/l_n \geq 2$, the A_n ion has an effect on the orientation of the magnetic moment of the adjacent magnetic ion only, and the j_n^s calculation will have to be performed in accordance with formula (3).

One should mention that, during calculation of the J_{ij}^s value, it is necessary to additionally take into account the

contribution from a direct interaction j^D , if the distance between the magnetic ions $d(M_i-M_j)$ is less than two diameters of these ions:

$$J_{ij}^s = \sum_n j_n^s + j^D. \quad (5)$$

The analysis of the relation between magnetic and crystal chemistry parameters in low-dimensional copper compounds, in which Cu^{2+} are located at short distances, has brought us to the above conclusion and allowed us to obtain the expression for the j^D calculation [29].

We based our considerations on the assumption that there exists some critical distance D_c between the magnetic ions when the AF and FM contributions from a direct interaction are equal and eliminate each other. Deviation from D_c results in AF coupling in the case of lower values and in FM coupling in the case of higher values. The value of the j^D contribution is proportional to the deviation value $(d(M_i-M_j) - D_c)$ and is in inverse proportion to the radii of magnetic ions r_{M_n} and the distance between them $d(M_i-M_j)$:

$$j^D = \frac{d(M_i-M_j) - D_c}{r_{M_n} d(M_i-M_j)}. \quad (6)$$

We have empirically found the D_c value for Cu^{2+} ions ($D_c = 2.88 \text{ \AA}$).

To calculate the sign and value of the strength of the magnetic interaction J_{ij}^s we have developed the ‘MagInter’ program. The program utilizes the expressions (1)–(4) obtained within the scope of this method. The geometric parameters used in these expressions ($h(A_n)$, $\Delta h(A_n)$, l_n and l'_n) are calculated from the interatomic distances and angles which, in turn, can be found through application of the program SELXTL [33]. The initial structural data format for the program (crystallographic parameters, atom coordinates) corresponds to that of the crystallographic information file (CIF) in the Inorganic Crystal Structure Database (ICSD) (FIZ Karlsruhe, Germany). Besides, in the calculations we used the ionic radii determined by Shannon [34].

The determined parameters of magnetic interactions are displayed only in cases when there are no restrictions for their simultaneous existence due to geometric configurations in the magnetic ion sublattices. The presence of specific configurations of magnetic ions results in geometric frustration of magnetic interactions. For non-stoichiometric compounds one should additionally take into account the presence of vacancies.

2.1. Critical positions of intermediate ions

There exist several critical positions of intermediate A_n ions when even a slight deviation from them could result in reorientation of magnetic moments (AF–FM transition) and/or dramatic change of the magnetic interaction strength. It appears important to note that, under the effects of temperature, pressure, magnetic field, etc, the ions in a crystal structure could undergo displacement. That is why during prediction of possible changes in the sign and strength of magnetic

interactions one should take into account not only the ions located exactly at critical positions, but also those in adjacent areas.

The following intermediate ion positions can be considered as critical:

- (a) $h(A_n) = r_M + r_{A_n}$: the distance $h(A_n)$ from the A_n ion center to the bond line M_i-M_j is equal to the sum of the M and A_n ionic radii. The A_n ion reaches the surface of a cylinder of radius r_M , limiting the space area between the magnetic ions M_i and M_j . In this case the A_n ion does not induce the emerging of a magnetic interaction. However, on a slight decrease of $h(A_n)$ (the A_n ion displacement inside this area) there emerges a strong FM interaction between magnetic ions.
- (b) $h(A_n) = r_{A_n}$ ($\Delta h(A_n) = 0$): the distance $h(A_n)$ from the center of the A_n ion to the bond line M_i-M_j is equal to the A_n ionic radius (the A_n reaches the bond line M_i-M_j). In this case the interaction between magnetic fields disappears. However, on a slight decrease of $h(A_n)$ (overlapping of the bond line by the A_n ion) there emerges a weak AF interaction, while on a slight increase of $h(A_n)$ (formation of a gap between the A_n ion and the bond line M_i-M_j) there emerges a weak FM interaction.
- (c) $l'_n/l_n = 2$: the A_n ion is located at the boundaries of the central one-third of the space between magnetic fields. In this case the insignificant displacement of the A_n ion to the center in parallel to the bond line M_i-M_j results in a dramatic increase of the magnetic interaction strength.

In the case when there are several intermediate A_n ions between the magnetic ions M_i and M_j , the following critical positions are possible:

- (d) When the ratio between the sums of the j_n^s contributions to the AF and FM components of the interaction becomes close to 1, the interaction between the magnetic ions M_i and M_j is weak, and a slight displacement of even one of the intermediate A_n ions could result in its complete disappearance or the AF–FM transition.
- (e) When even one of the intermediate A_n ions is in a critical position of (a) or (c) type, the contribution to AF or FM components of the interaction could undergo dramatic changes because of even a slight displacement of these ions and, therefore, cause changes of respective scale in the interaction strength and reorientation of magnetic ion spins.

The sign and strength of magnetic couplings in paraelectric phases of TbMn_2O_5 and BiMn_2O_5 as well as in magnetically ordered non-polar and polar models of these compounds were calculated using the program ‘MagInter’. The structural data for TbMn_2O_5 at room temperature [35] and BiMn_2O_5 at room temperature [36] and $T = 100$ K [11] were taken for calculations and model development. Besides, in the above calculations we used the ionic radii determined by Shannon [34] ($r_{\text{Mn}^{3+}} = 0.53$ Å (coordination number CN is equal to 5), $r_{\text{Mn}^{4+}} = 0.58$ Å (CN = 6) and $r_{\text{O}^{2-}} = 1.40$ Å). The contribution from the direct interaction between manganese ions j^D was not taken into account, since all the distances

between manganese in these compounds are longer than two Mn ion diameters. The bond valences of manganese ions $V_{\text{Mn}^{3+}}$ and $V_{\text{Mn}^{4+}}$ were calculated by Brese and O’Keeffe [37]. The structural parameters, bond distances and bond valences of Mn^{3+} and Mn^{4+} ions in TbMn_2O_5 , BiMn_2O_5 and models are presented in tables 1 and 2. The parameters of the main magnetic interactions in these compounds and models are presented in tables 3 and 4.

3. Results and discussion

3.1. Characterization of magnetic interactions and their competition in paraelectric phases of TbMn_2O_5 and BiMn_2O_5

The compounds TbMn_2O_5 [35] and BiMn_2O_5 [11, 36] in the paraelectric phase crystallize in a centrosymmetrical orthorhombic space group $Pbam$ and have two types of magnetic ions: Mn1 (Mn^{4+} , $S = 3/2$) in distorted oxygen octahedra Mn^{4+}O_6 and Mn2 (Mn^{3+} , $S = 2$) in distorted square pyramids Mn^{3+}O_5 (figures 2(a) and (b)). The Mn^{4+}O_6 octahedra are coupled alternately by common edges O2–O2 and O3–O3 into a linear chain along the c axis. The Mn^{3+}O_5 pyramids are coupled into dimers by the common edge O1–O1. These dimers couple the octahedra chains along the a axis through the ions O3 located in the pyramid vertices and along the b axis through the ions O4 located in the pyramid bases.

According to our calculations, in the paraelectric phases of TbMn_2O_5 and BiMn_2O_5 at room temperature and $T = 100$ K the respective magnetic couplings between manganese ions are of the same sign and differ insignificantly in strength (tables 3 and 4; figures 2(d), 3(a) and (b)). The compound BiMn_2O_5 at room temperature and at 100 K are referred to as Bi–RT and Bi–LT, respectively.

Strong AF J_1 and J_2 couplings alternate in the linear chain along the c axis (figure 2(d)). The J_1 coupling is weaker than the J_2 coupling (the ratio of intra-chain couplings $J_2/J_1 = 1.45$ (1.27 and 1.31) in $\text{Tb}(\text{Bi–RT and Bi–LT})$ systems). The main contribution to the AF components of the J_1 and J_2 couplings is provided by two O2 ions (the value of the contributions from two O2 ions: $2j_{\text{O}2} = -0.059(-0.058$ and $-0.058)$ Å $^{-1}$) and two O3 ions ($2j_{\text{O}3} = -0.077(-0.070$ and $-0.072)$ Å $^{-1}$), respectively. Higher values of these AF contributions result from the fact that the O2 and O3 ions are located in the central one-third part of the space between magnetic ions ($l'/l = 1$). However, the O2 and O3 ion positions are close to the critical position ‘b’ (see section 2), since the distances from these ions to the bond line Mn1–Mn1 ($h(\text{O}2) = 1.27$ Å and $h(\text{O}3) = 1.26$ – 1.27 Å) are slightly less than the oxygen ion radius ($r_{\text{O}^{2-}} = 1.40$ Å), i.e. the ions O2 and O3 slightly overlap the bond line Mn1–Mn1.

Slight O2 and O3 ion displacements perpendicular to the bond line Mn1–Mn1 could control the spin orientation of the J_1 and J_2 couplings. The contributions of O2 and O3 ions to the J_1 and J_2 couplings disappear, if $h(\text{O}2)$ and $h(\text{O}3)$ increase by 0.13–0.14 Å and reach 1.40 Å. During further removal of these ions from the bond line the character of their contribution changes into a ferromagnetic one and, as a result, the J_1 and J_2 couplings undergo the AF \rightarrow FM transition.

Table 1. Structural parameters, bond distances and bond valences of Mn1 and Mn2 ions (V_{Mn1} , V_{Mn2}) in TbMn_2O_5 .

TbMn_2O_5	Alonso [35]	M-DO ^a model	P-Mn2 ^b model		P-O1 ^c model ^c		Wang [7, 8] ^d	
Space group	<i>Pbam</i>	<i>Pbam</i>	<i>Pb2₁m</i>		<i>Pb2₁m</i>		<i>Pb2₁m</i> N26	
<i>a</i> (Å)	7.3251	7.317	7.317		7.317		7.3014	
<i>b</i> (Å)	8.5168	8.506	8.506		8.506		8.5393	
<i>c</i> (Å)	5.6750	5.660	5.660		5.660		5.6056	
Mn^{4+}O_6	Mn1	Mn1	Mn1		Mn1		Mn1	
Mn1–O2(x2) (Å)	1.954	2.013	2.013		2.013		1.923(O2, O2')	
Mn1–O3(x2) (Å)	1.847	2.013	2.013		2.013		1.871(O3, O3')	
Mn1–O4(x2) (Å)	1.912	1.908	1.791(O4); 1.808 (O4')		1.791(O4); 1.826 (O4')		1.923(O4); 1.937(O4')	
V_{Mn1}	4.01	3.30	3.75		3.70		3.96	
Mn^{3+}O_5	Mn2	Mn2	Mn2	Mn2'	Mn2	Mn2'	Mn2	Mn2'
Mn2–O1(x2) (Å)	1.927	1.928	1.915(O1)	1.942(O1)	1.915(O1)	1.942(O1)	1.919(O1)	1.928(O1)
Mn2–O3(x1) (Å)	2.021	1.805	1.797(O3)	1.813(O3')	1.805(O3)	1.805(O3')	1.908(O3)	1.912(O3')
Mn2–O4(x2) (Å)	1.890	1.855	1.956(O4)	1.915(O4')	1.942(O4)	1.915(O4')	1.914(O4)	1.911(O4')
V_{Mn2}	3.18	3.70	3.40	3.40	3.42	3.42	3.29	3.26
Mn1: <i>x</i>	0	0	0.2500		0.2500		0.2501	
<i>y</i>	1/2	1/2	0.5000		0.5000		0.5003	
<i>z</i>	0.2618	0.2557	0.2557		0.2557		0.2558	
Mn2(Mn2'): <i>x</i>	0.4120	0.4114	0.6614(0.1614)		0.6614(0.1614)		0.6512 (0.1516)	
<i>y</i>	0.3510	0.3505	0.3529(0.1519)		0.3505(0.1495)		0.3558 (0.1456)	
<i>z</i>	1/2	1/2	1/2 (1/2)		1/2 (1/2)		1/2 (1/2)	
O1: <i>x</i>	0	0	0.2500		0.2500		0.2508	
<i>y</i>	0	0	0.0000		-0.0024		0.0002	
<i>z</i>	0.2710	0.2710	0.2710		0.2710		0.2709	
O2(O2'): <i>x</i>	0.1617	0.1808	0.4308(0.9308)		0.4308(0.9308)		0.4146 (0.9148)	
<i>y</i>	0.4463	0.4463	0.4463(0.0537)		0.4463(0.0537)		0.4480 (0.0517)	
<i>z</i>	0	0	0(0)		0(0)		0 (0)	
O3(O3'): <i>x</i>	0.1528	0.1838	0.4338(0.9338)		0.4338(0.9338)		0.4060 (0.9071)	
<i>y</i>	0.4324	0.4324	0.4324(0.0676)		0.4324(0.0676)		0.4329 (0.0655)	
<i>z</i>	1/2	1/2	1/2 (1/2)		1/2 (1/2)		1/2 (1/2)	
O4(O4'): <i>x</i>	0.3973	0.3973	0.6473(0.1473)		0.6473(0.1473)		0.6477 (0.1459)	
<i>y</i>	0.2062	0.2062	0.1911(0.3067)		0.1911(0.3043)		0.2077 (0.2919)	
<i>z</i>	0.2483	0.2550	0.2550(0.7450)		0.2550(0.7450)		0.2438 (0.7579)	

^a Magnetic ordering and elimination of dipole moments of Mn1O_6 octahedra.

^b Spontaneous polarization along the *b* axis accompanied by the Mn2, Mn2', O4 and O4' ion displacements.

^c Spontaneous polarization along the *b* axis accompanied by the O1, O4 and O4' ion displacements.

^d Coordinates of all TbMn_2O_5 atoms from [7, 8] are displaced by 1/4 along the *x* axis to preserve the structural motif.

Aside from two O2 ions, the J_1 coupling space contains four O4 ions which initiate the emerging of slight contributions to the FM component of this interaction, since they are removed from the middle of the Mn1–Mn1 straight line to the Mn1 ions. Moreover, the O4 ions are located near the boundary of the interaction space (the critical position 'a') and, in the case of their displacement perpendicular to the chain (along the *b* axis) by as little as 0.01–0.02 Å from the line Mn1–Mn1, they leave the boundaries and cannot participate in the J_1 coupling formation. However, the O4 ions have a leading role in coupling with the second (J_2), third (J_3) and fourth (J_4) neighbors in the linear chain along the *c* axis, since they appear in the central one-third of these interaction spaces.

The J_2 couplings are ferromagnetic and weaker than the AF J_1 couplings (the ratio J_2/J_1 is equal to -0.47 (-0.44 and -0.44) in $\text{Tb}(\text{Bi-RT}$ and Bi-LT) systems), since the O4 ions reduce the comparatively large AF contribution j_{Mn1} ($j_{\text{Mn1}} = -0.033$ (-0.032 and -0.032) Å⁻¹ in $\text{Tb}(\text{Bi-RT}$ and Bi-LT) systems) of the intermediate Mn1 ion and small AF contributions of the two intermediate ions O2 and O3. However, in the case of the O4 ions leaving the interaction space the J_2 couplings will undergo the phase transition

FM \rightarrow AF ($J_2/J_1 = 0.66$) and compete with the J_1 and J_2 couplings.

The J_3 and $J_{3'}$ couplings between the third neighbors in the chain are not equivalent (tables 3 and 4; figure 2(d)). The J_3 coupling is very weak ($J_3/J_1 = 0.04$), belongs to the AF type and does not compete with the nearest couplings of the chain. Alternatively, the $J_{3'}$ coupling is of the FM type ($J_{3'}/J_1 = -0.47$ (-45 and -45) in $\text{Tb}(\text{Bi-RT}$ and Bi-LT) systems) and competes with the nearest J_1 and J_2 couplings. However, in the local space of the J_3 and $J_{3'}$ couplings the locations of the O4 ions providing the highest contribution to the FM component of these interactions are critical in regard to displacements in two directions: perpendicular (critical position 'a') and parallel (critical position 'c') to the chain. Removal of the O4 ions beyond the interaction space boundary at slight displacement (by 0.02 Å) along the *b* axis increases the strength of the AF J_3 coupling ($J_3/J_1 = 0.27$ (0.28)), transforms the $J_{3'}$ coupling from the FM type to the AF type ($J_{3'}/J_1 = 0.75$ (0.72 and 0.072) in $\text{Tb}(\text{Bi-RT}$ and Bi-LT) systems) and, thus, eliminates its competition with the nearest-neighbor interactions. Significant changes in the J_3 and $J_{3'}$ couplings at slight displacements of the O4 ions in parallel

Table 2. Structural parameters, bond distances and bond valences of Mn1 and Mn2 ions (V_{Mn1} , V_{Mn2}) in BiMn_2O_5 .

BiMn_2O_5	Munoz [36]	Granado [11]	M-DO ^a model	P-Mn2 ^b model		P-O1 ^c model	
Space group	<i>Pbam</i>	<i>Pbam</i>	<i>Pbam</i>	<i>Pb2₁m</i>		<i>Pb2₁m</i>	
<i>a</i> (Å)	7.5608	7.541 16	7.541 16	7.541 16		7.541 16	
<i>b</i> (Å)	8.5330	8.529 94	8.529 94	8.529 94		8.529 94	
<i>c</i> (Å)	5.7607	5.754 37	5.754 37	5.754 37		5.754 37	
Mn^{4+}O_6	Mn1	Mn1	Mn1	Mn1		Mn1	
Mn1–O2(x2) (Å)	1.968	1.961	2.047	2.047		2.047	
Mn1–O3(x2) (Å)	1.870	1.872	2.047	2.047		2.047	
Mn1–O4(x2) (Å)	1.910	1.922	1.922	1.765(O4); 1.818(O4')		1.765(O4); 1.864(O4')	
V_{Mn1}	3.88	3.86	3.07	3.61		3.52	
Mn^{3+}O_5	Mn2	Mn2	Mn2	Mn2	Mn2'	Mn2	Mn2'
Mn2–O1(x2) (Å)	1.899	1.897	1.897	1.894(O1)	1.961(O1)	1.894(O1)	1.961(O1)
Mn2–O3(x1) (Å)	2.085	2.086	1.820	1.803(O3)	1.838(O3')	1.820(O3)	1.820(O3')
Mn2–O4(x2) (Å)	1.929	1.916	1.916	2.075(O4)	1.952(O4')	2.038(O4)	1.952(O4')
V_{Mn2}	3.06	3.11	3.54	3.14	3.16	3.19	3.20
Mn1: <i>x</i>	1/2	1/2	1/2	0.7500		0.7500	
<i>y</i>	0	0	0	0.0000		0.0000	
<i>z</i>	0.2613	0.2596	0.259 6	0.2596		0.2596	
Mn2(Mn2'): <i>x</i>	0.4074	0.407 55	0.407 55	0.657 55(0.157 55)		0.657 55(0.157 55)	
<i>y</i>	0.3516	0.350 91	0.350 91	0.356 91(0.155 09)		0.350 91(0.149 09)	
<i>z</i>	1/2	1/2	1/2	1/2(1/2)		1/2(1/2)	
O1: <i>x</i>	0	0	0	0.2500		0.2500	
<i>y</i>	0	0	0	0.0000		–0.0060	
<i>z</i>	0.2866	0.2876	0.2876	0.2795		0.2795	
O2(O2'): <i>x</i>	0.1553	0.1567	0.1750	0.4250(0.9250)		0.4250(0.9250)	
<i>y</i>	0.4440	0.4453	0.4453	0.4453(0.0547)		0.4453(0.0547)	
<i>z</i>	0	0	0	0(0)		0(0)	
O3(O3'): <i>x</i>	0.1440	0.1437	0.1809	0.4309(0.9309)		0.4309(0.9309)	
<i>y</i>	0.4241	0.4243	0.4243	0.4243(0.0757)		0.4243(0.0757)	
<i>z</i>	1/2	1/2	1/2	1/2(1/2)		1/2(1/2)	
O4(O4'): <i>x</i>	0.3856	0.3866	0.3866	0.6366(0.1366)		0.6366(0.1366)	
<i>y</i>	0.1995	0.2018	0.2018	0.1810(0.3120)		0.1810(0.3059)	
<i>z</i>	0.2539	0.2525	0.2525	0.2525(0.7455)		0.2525(0.7455)	

^a Magnetic ordering and elimination of dipole moments of Mn1O_6 octahedra.

^b Spontaneous polarization along the *b* axis accompanied by the Mn2, Mn2', O4 and O4' ion displacements.

^c Spontaneous polarization along the *b* axis accompanied by the O1, O4 and O4' ion displacements.

to the chain result from the fact that these ions are located near (l'/l approximately equal 2) the boundary of the central one-third part of the local space of these interactions. In the J_3 coupling the O4 ions are located beyond, while in the $J_{3'}$ coupling they are located inside, the central part of the interaction space. The displacement (by 0.02(0.04) Å in Tb(Bi) systems) of the O4 ions into the central part of the J_3 coupling and the accompanying removal of these ions from the central part of the $J_{3'}$ coupling result in the transition of the J_3 coupling into the FM state ($J_3/J_1 = -1.13$ (–1.02 and –1.04) in Tb(Bi–RT and Bi–LT) systems) and the $J_{3'}$ coupling into the AF state ($J_{3'}/J_1 = 0.57$ (0.51) in Tb(Bi) systems). In this case there is still competition in the chain, but exclusively due to the J_3 couplings.

The J_4 coupling strength attains zero ($J_4/J_1 = 0$ (0 and –0.02) in Tb(Bi–RT and Bi–LT) systems), since the sum of contributions of three intermediate Mn1 ions, four O2 ions and two O3 ions to the AF component of the interaction is approximately equal to the sum of eight O4 ions to the interaction FM component. In Tb and Bi–HT systems these contributions eliminate each other while in the Bi–RT system the FM contribution is slightly higher than the AF contribution. However, in the case of slight displacement of the O4 ions from

the line –Mn1–Mn1– beyond the boundary of the interaction space the J_4 coupling will be transformed into a comparatively strong AF coupling ($J_4/J_1 = 0.36$ –0.40) and compete with the nearest couplings in the chain.

The AF intra-dimer J_5 coupling is formed under the effect of two intermediate O1 ions localized in the center between the Mn2 ions ($l'/l = 1$) at a distance $h(\text{O1}) = 1.300$ (1.229 and 1.222) Å from the O1 ion center to the straight line Mn2–Mn2. Each O1 ion contributes -0.025 (–0.041 and –0.042) Å^{–1} to the emerging of the AF component of the J_5 coupling in Tb(Bi–RT and Bi–LT) systems. As a result, the J_5 coupling in the Tb system is markedly weaker ($J_5^{\text{Tb}}/J_5^{\text{Bi-HT}} = 0.61$, $J_5^{\text{Tb}}/J_5^{\text{Bi-LT}} = 0.59$) than in the Bi system. The O1 ions are located in the critical position 'b' and could control the strength and sign of the J_5 coupling. The intra-dimer coupling could disappear, if $h(\text{O1})$ increases up to 1.40 Å, or changes the sign to the opposite, if $h(\text{O1})$ surpasses this value.

In the *ab* plane (figures 2(a), 3(a) and (b)) the linear chains –Mn1–Mn1– and dimers Mn2–Mn2 are coupled by the strong AF J_3 (along the *b* axis) and J_4 (along the *a* axis) couplings ($J_1 = 0.7$ (0.8) $J_2 = 1.1$ (0.7) $J_5 = 0.7$ (0.8) $J_3 = 0.6$ (0.7) J_4 in the Tb(Bi) system). The J_3 coupling emerges mainly under the effect of one intermediate O4 ion localized

Table 3. Parameters of magnetic coupling in TbMn₂O₅ calculated on the basis of structural data.

TbMn ₂ O ₅	Alonso [35]	M-DO ^a model	P-Mn2 ^b model	P-O1 ^c model	Wang [7, 8]
Space group	<i>Pbam</i>	<i>Pbam</i>	<i>Pb2₁m</i>	<i>Pb2₁m</i>	<i>Pb2₁m</i>
<i>a</i> (Å)	7.3251	7.317	7.317	7.317	7.3014
<i>b</i> (Å)	8.5168	8.506	8.506	8.506	8.5393
<i>c</i> (Å)	5.6750	5.660	5.660	5.660	5.6056
<i>d</i> (Mn1–Mn1) (Å)	2.971	2.895	2.895	2.895	2.868
<i>J</i> ^{<i>s</i>} ₁ (Å ⁻¹)	-0.059 ^d , -0.053	0	0	0	-0.058 ^d , -0.055
<i>d</i> (Mn1–Mn1) (Å)	2.704	2.765	2.765	2.765	2.738
<i>J</i> ^{<i>s</i>} ₂ (Å ⁻¹)	-0.077	0.033	0.033	0.033	-0.066
<i>d</i> (Mn1–Mn1) (Å)	5.675	5.660	5.660	5.660	5.606
<i>J</i> ^{<i>s</i>} ₂ = <i>J</i> ^{<i>s</i>} _{c1} (Å ⁻¹)	-0.039 ^d , 0.025	0.032	0.018	0.019	-0.039 ^d , -0.006
<i>d</i> (Mn1–Mn1) (Å)	8.379	8.425	8.425	8.425	8.343
<i>J</i> ^{<i>s</i>} ₃ (Å ⁻¹)	-0.016 ^{d,e} , -0.002 ^e , -0.016 ^{d,f} , 0.060 ^f	0.007	0.004	0.005	-0.016 ^d , 0.022
<i>d</i> (Mn1–Mn1) (Å)	8.646	8.555	8.555	8.555	8.473
<i>J</i> ^{<i>s</i>} _{3'} (Å ⁻¹)	-0.044 ^{d,e} , -0.030 ^e , -0.044 ^{d,f} , 0.025 ^f	0.036	0.022	0.023	-0.045 ^d , -0.037
<i>d</i> (Mn1–Mn1) (Å)	11.350	11.320	11.320	11.320	11.211
<i>J</i> ^{<i>s</i>} ₄ (Å ⁻¹)	-0.021 ^d , 0.000	0.012	0.008	0.008	-0.021 ^d , -0.010
<i>d</i> (Mn1–Mn2) (Å)	3.344	3.350	3.368 (3.332)	3.350 (3.350)	3.407 (3.401)
<i>J</i> ^{<i>s</i>} ₃ (<i>J</i> ^{<i>s</i>} _{3'}) (Å ⁻¹)	-0.071	-0.078	-0.081 (-0.082)	-0.082 (-0.081)	-0.071 (-0.068)
<i>d</i> (Mn1–Mn2) (<i>d</i> (Mn1–Mn2')) (Å)	3.542	3.548	3.541 (3.556)	3.548 (3.548)	3.460 (3.466)
<i>J</i> ^{<i>s</i>} ₄ (<i>J</i> ^{<i>s</i>} _{4'}) (Å ⁻¹)	-0.085	-0.095	-0.095 (-0.094)	-0.095 (-0.094)	-0.093 (-0.093)
<i>d</i> (Mn2–Mn2) (Å)	2.847	2.855	2.855	2.855	2.863
<i>J</i> ^{<i>s</i>} ₅ (Å ⁻¹)	-0.050	-0.051	-0.051	-0.051	-0.057
<i>d</i> (Mn1–Mn2) (<i>d</i> (Mn1–Mn2')) (Å)	5.295	5.254	5.266 (5.242)	5.254 (5.254)	5.262 (5.257)
<i>J</i> ^{<i>s</i>} ₆ (<i>J</i> ^{<i>s</i>} _{6'}) (Å ⁻¹)	-0.081	-0.081	-0.071 (-0.075)	-0.073 (-0.075)	-0.084 (-0.084)
<i>d</i> (Mn1–Mn2) (<i>d</i> (Mn1–Mn2')) (Å)	5.423	5.383	5.378 (5.388)	5.383 (5.383)	5.296 (5.300)
<i>J</i> ^{<i>s</i>} ₇ (<i>J</i> ^{<i>s</i>} _{7'}) (Å ⁻¹)	-0.094	-0.087	-0.086 (-0.086)	-0.086 (-0.086)	-0.095 (-0.095)
<i>d</i> (Mn2–Mn2) (Å)	6.116	6.102	6.102	6.102	6.233
<i>J</i> ^{<i>s</i>} ₈ (Å ⁻¹)	-0.020 ^d , -0.018	0.005	0.005	0.005	-0.015
<i>d</i> (Mn1–Mn1) (Å)	5.617	5.610	5.610	5.610	5.617; 5.619
<i>J</i> ^{<i>s</i>} _{sq} (Å ⁻¹)	-0.007	-0.008	-0.009	-0.009	-0.007; -0.007
<i>d</i> (Mn1–Mn1) (Å)	7.325	7.317	7.317	7.317	7.301
<i>J</i> ^{<i>s</i>} _{a1} (Å ⁻¹)	-0.047	-0.046	-0.046	-0.046	-0.046
<i>d</i> (Mn1–Mn1) (Å)	8.517	8.506	8.506	8.506	8.539
<i>J</i> ^{<i>s</i>} _{b1} (Å ⁻¹)	-0.040	-0.040	-0.040	-0.040	-0.039
<i>d</i> (Mn2–Mn2) (<i>d</i> (Mn2'–Mn2')) (Å)	7.325	7.317	7.317 (7.317)	7.317 (7.317)	7.301 (7.301)
<i>J</i> ^{<i>s</i>} _{a2} (<i>J</i> ^{<i>s</i>} _{a2'}) (Å ⁻¹)	0.023	0.021	0.018 (0.019)	0.019 (0.018)	0.023 (0.023)
<i>d</i> (Mn2–Mn2) (<i>d</i> (Mn2'–Mn2')) (Å)	8.517	8.506	8.506 (8.506)	8.506 (8.506)	8.539 (8.539)
<i>J</i> ^{<i>s</i>} _{b2} (<i>J</i> ^{<i>s</i>} _{b2'}) (Å ⁻¹)	-0.024	0.012	0.012 (0.012)	0.012 (0.012)	-0.025 (-0.025)
<i>d</i> (Mn2–Mn2) (<i>d</i> (Mn2'–Mn2')) (Å)	5.675	5.660	5.660 (5.660)	5.660 (5.660)	5.606 (5.606)
<i>J</i> ^{<i>s</i>} _{c2} (<i>J</i> ^{<i>s</i>} _{c2'}) (Å ⁻¹)	-0.003	0.027	0.029 (0.029)	0.029 (0.029)	0.029 (0.030)

^a Magnetic ordering and elimination of dipole moments of Mn1O₆ octahedra.

^b Spontaneous polarization along the *b* axis accompanied by the Mn2, Mn2', O4 and O4' ion displacements.

^c Spontaneous polarization along the *b* axis accompanied by the O1, O4 and O4' ion displacements.

^d During calculation of the *J_n* coupling the contribution from an intermediate ion located in the critical position 'a' was not taken into account.

^e During calculation of the *J_n* coupling the formula (3) is taken, since some intermediate ions are localized in the critical position 'c'.

^f During calculation of the *J_n* coupling the formula (2) is taken, since some intermediate ions are localized in the critical position 'c'.

in the central one-third part of the space (*l*'/*l* ≈ 1 between the ions Mn1 and Mn2 at a distance *h*(O4) = 0.905–0.919 Å from the straight line Mn1–Mn2 and makes a substantial

contribution *j*_{O4} (*j*_{O4} = -0.089(-0.085) Å⁻¹ in the Tb(Bi) system) to the interaction AF component. The *J*₃ coupling value slightly reduces due to a small contribution of two

Table 4. Parameters of magnetic coupling in BiMn₂O₅ calculated on the basis of structural data.

BiMn ₂ O ₅	Munoz [36]	Granado [11]	M-DO ^a model	P-Mn2 ^b model	P-O1 ^c model
Space group	<i>Pbam</i>	<i>Pbam</i>	<i>Pbam</i>	<i>Pb2₁m</i>	<i>Pb2₁m</i>
<i>a</i> (Å)	7.5608	7.541 16	7.541 16	7.541 16	7.541 16
<i>b</i> (Å)	8.5330	8.529 94	8.529 94	8.529 94	8.529 94
<i>c</i> (Å)	5.7607	5.754 37	5.754 37	5.754 37	5.754 37
<i>d</i> (Mn1–Mn1) (Å)	3.011	2.988	2.988	2.988	2.988
<i>J</i> ^s 1 (Å ⁻¹)	-0.058 ^d , -0.055	-0.058 ^d , -0.055	0.003	0.002	0.002
<i>d</i> (Mn1–Mn1) (Å)	2.750	2.767	2.767	2.767	2.767
<i>J</i> ^s 2 (Å ⁻¹)	-0.070	-0.072	0.057	0.057	0.057
<i>d</i> (Mn1–Mn1) (Å)	5.761	5.754	5.754	5.754	5.754
<i>J</i> ₂ ^s = <i>J</i> _{c1} ^s (Å ⁻¹)	-0.038 ^d , 0.024	-0.038 ^d , 0.026	0.033	0.017	0.020
<i>d</i> (Mn1–Mn1) (Å)	8.511	8.521	8.521	8.521	8.521
<i>J</i> ₃ ^s (Å ⁻¹)	-0.016 ^{d,e} , -0.002 ^e , -0.016 ^{d,f} , 0.056 ^f	-0.016 ^{d,e} , -0.002 ^e , -0.016 ^{d,f} , 0.057 ^f	0.008	0.005	0.005
<i>d</i> (Mn1–Mn1) (Å)	8.771	8.742	8.742	8.742	8.742
<i>J</i> ₃ ^s (Å ⁻¹)	-0.042 ^{d,e} , -0.028 ^e , -0.042 ^{d,f} , 0.024 ^f	-0.043 ^{d,e} , -0.028 ^e , -0.043 ^{d,f} , 0.025 ^f	0.040	0.023	0.025
<i>d</i> (Mn1–Mn1) (Å)	11.521	11.509	11.509	11.509	11.509
<i>J</i> ₄ ^s (Å ⁻¹)	-0.020 ^d , 0.000	-0.021 ^d , 0.001	0.014	0.009	0.010
<i>d</i> (Mn1–Mn2) (Å)	3.374	3.370	3.370	3.416 (3.325)	3.370 (3.370)
<i>J</i> ^s 3 (<i>J</i> ^s 3') (Å ⁻¹)	-0.067	-0.067	-0.064	-0.066 (-0.070)	-0.068 (-0.067)
<i>d</i> (Mn1–Mn2) (<i>d</i> (Mn1–Mn2')) (Å)	3.603	3.602	3.602	3.585 (3.621)	3.602 (3.602)
<i>J</i> ^s 4 (<i>J</i> ^s 4') (Å ⁻¹)	-0.080 ^d , -0.076	-0.080 ^d , -0.076	-0.091	-0.095 (-0.089)	-0.090 (-0.090)
<i>d</i> (Mn2–Mn2) (Å)	2.894	2.901	2.901	2.901	2.901
<i>J</i> ^s 5 (Å ⁻¹)	-0.082	-0.085	-0.085	-0.062	-0.062
<i>d</i> (Mn1–Mn2) (<i>d</i> (Mn1–Mn2')) (Å)	5.360	5.343	5.343	5.372 (5.315)	5.343 (5.343)
<i>J</i> ^s 6 (<i>J</i> ^s 6') (Å ⁻¹)	-0.071	-0.073	-0.071	-0.058 (-0.067)	-0.060 (-0.067)
<i>d</i> (Mn1–Mn2) (<i>d</i> (Mn1–Mn2')) (Å)	5.507	5.493	5.493	5.481 (5.505)	5.493 (5.493)
<i>J</i> ^s 7 (<i>J</i> ^s 7') (Å ⁻¹)	-0.093	-0.093	-0.085	-0.084 (-0.084)	-0.084 (-0.084)
<i>d</i> (Mn2–Mn2) (Å)	6.162	6.147	6.147	6.147	6.147
<i>J</i> ^s 8 (Å ⁻¹)	-0.019	-0.019	0.011	0.011	0.011
<i>d</i> (Mn1–Mn1) (Å)	5.700	5.693	5.693	5.693	5.693
<i>J</i> _{sq} ^s (Å ⁻¹)	-0.008	-0.008	-0.009	-0.010	-0.009
<i>d</i> (Mn1–Mn1) (Å)	7.561	7.541	7.541	7.541	7.541
<i>J</i> _{a1} ^s (Å ⁻¹)	-0.041	-0.040	-0.040	-0.042	-0.042
<i>d</i> (Mn1–Mn1) (Å)	8.533	8.530	8.530	8.530	8.530
<i>J</i> _{b1} ^s (Å ⁻¹)	-0.037	-0.036	-0.038	-0.039	-0.039
<i>d</i> (Mn2–Mn2) (<i>d</i> (Mn2'–Mn2')) (Å)	7.561	7.541	7.541	7.541 (7.541)	7.541 (7.541)
<i>J</i> _{a2} ^s (<i>J</i> _{a2'} ^s) (Å ⁻¹)	0.021	0.022	0.024	0.019 (0.022)	0.021 (0.021)
<i>d</i> (Mn2–Mn2) (<i>d</i> (Mn2'–Mn2')) (Å)	8.533	8.530	8.530	8.530 (8.530)	8.530 (8.530)
<i>J</i> _{b2} ^s (<i>J</i> _{b2'} ^s) (Å ⁻¹)	-0.027	-0.027	-0.021	-0.020 (-0.021)	-0.020 (-0.020)
<i>d</i> (Mn2–Mn2) (<i>d</i> (Mn2'–Mn2')) (Å)	5.761	5.754	5.754	5.754 (5.754)	5.754 (5.754)
<i>J</i> _{c2} ^s (<i>J</i> _{c2'} ^s) (Å ⁻¹)	-0.001	-0.002	0.031	0.033 (0.034)	0.033 (0.033)

^a Magnetic ordering and elimination of dipole moments of Mn1O₆ octahedra.

^b Spontaneous polarization along the *b* axis accompanied by the Mn2, Mn2', O4 and O4' ion displacements.

^c Spontaneous polarization along the *b* axis accompanied by the O1, O4 and O4' ion displacements.

^d During calculation of the *J_n* coupling the contribution from an intermediate ion located in the critical position 'a' was not taken into account.

^e During calculation of the *J_n* coupling the formula (3) is taken, since some intermediate ions are localized in the critical position 'c'.

^f During calculation of the *J_n* coupling the formula (2) is taken, since some intermediate ions are localized in the critical position 'c'.

O3 ions and one O4 ion to this interaction ferromagnetic component. The *J*4 coupling is formed under the effect of the O3 ion (*l*'_{O3}/*l*_{O3} = 1.11(1.14); *h*(O3) = 0.777(0.819) Å in the

Tb(Bi) system) making a substantial AF contribution (*j*_{O3} = -0.100(-0.091) Å⁻¹) and an insignificant FM contribution from the O1, O2, O3 and O4 ions.

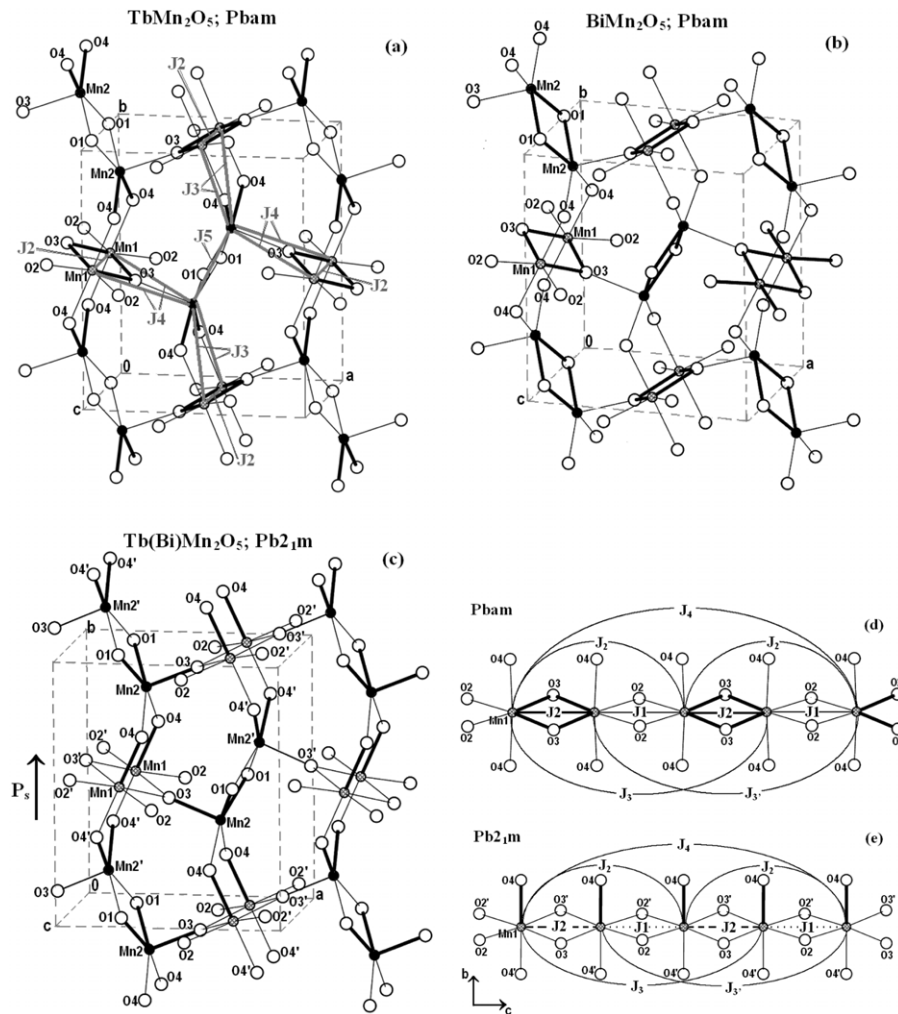


Figure 2. The relation of Mn–O bond lengths in Mn1 and Mn2 polyhedra: the crystal structure of the paraelectric phase of TbMn_2O_5 (a) and BiMn_2O_5 (b) and magnetically ordered ferroelectric model $\text{Tb(Bi)Mn}_2\text{O}_5$ at polar displacements of Mn2, Mn2', O4 and O4' (c). The linear chain along the c axis and the J_n coupling in the paraelectric phase (d) and for the magnetically ordered ferroelectric model (e). Thick and thin lines refer to short and long Mn–O bonds, respectively.

Besides the above interactions, more remote strong AF J_6 (along the b axis) and J_7 (along the a axis) couplings take place between linear chains and dimers. The J_7 coupling is a dominating interaction ($J_7/J_1 = 1.77(1.69)$ in the Tb(Bi) system) in all the compounds under consideration. The contribution (from -0.101 to -0.102 \AA^{-1}) to the AF component of this interaction emerges under the effect of one O2 ion located in the central one-third part of the interaction space ($l'_{O2}/l_{O2} = 1.78-1.71$), almost on the straight line Mn1–Mn2 ($h(\text{O}2) = 0.099-0.121 \text{ \AA}$). The J_6 coupling is weaker than the J_7 coupling ($J_6/J_7 0.86(0.76$ and $0.78)$ in the Tb(Bi–RT and Bi–LT) systems)), since the O4 ion, which initiates its formation, is located further from the line Mn1–Mn2 ($h(\text{O}4) = 0.391-0.493 \text{ \AA}$; $l'_{O4}/l_{O4} = 1.86-1.87$).

One should emphasize that, unlike the intra-chain J_1 , J_2 and J_n couplings and intra-dimer J_5 coupling, the J_3 , J_4 , J_6 and J_7 couplings are stable, since they do not contain intermediate ions in critical locations. Reorientation of the J_3 and J_6 coupling spins requires a substantial distortion of the crystal structure (O4 displacement along the x axis

$>0.5 \text{ \AA}$) while reorientation of the J_4 and J_7 coupling spins is impossible within the frames of given crystal structures.

All strong AF J_1 , J_2 , J_3 , J_4 , J_6 and J_7 couplings form geometrically frustrated isosceles $J_2J_3J_3$ and $J_2J_4J_4$ triangles or distorted $J_1J_3J_6$ and $J_1J_4J_7$ triangles (figures 3(a) and (b)). Besides, the J_3 , J_4 , J_6 and J_7 couplings compete with weaker inter-dimer AF J_8 and J_9 couplings in the triangles $J_8J_3J_3$, $J_8J_6J_6$, $J_9J_4J_4$ and $J_9J_7J_7$.

The Mn1 ion sublattice can be presented as an antiferromagnetic square lattice in the ab plane with competing interactions along the side (J_{sq}) and diagonal of the square (J_{a1} and J_{b1}). The value of frustration ratio of the second-neighbor (diagonal) coupling to the nearest-neighbor (side) coupling is significantly higher than the critical value ($\alpha = 1/2$) and falls into the range 4.5–6.7.

The arrangement of AF Mn2–Mn2 magnetic dimers in the ab planes is similar to that of Cu–Cu dimers in the compound $\text{SrCu}_2(\text{BO}_3)_2$ [38]. However, unlike $\text{SrCu}_2(\text{BO}_3)_2$, the inter-dimer couplings (J_{10} and J_{11}) in $\text{Tb(Bi)Mn}_2\text{O}_5$ are

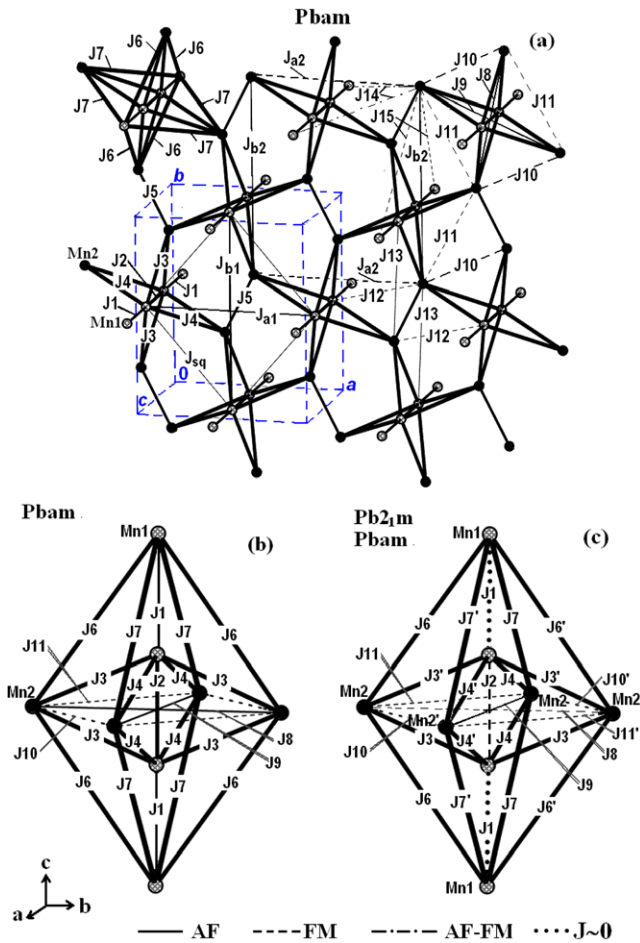


Figure 3. (a) The sublattice of Mn^{3+} ($Mn2$) and Mn^{4+} ($Mn1$) and the coupling J_n in the frustrated paraelectric phase of $Tb(Bi)Mn_2O_5$. Fragment of sublattice: change of the coupling J_n parameters at transition from frustrated paraelectric state (b) to magnetically ordered ferroelectric state (models M-DO, P-Mn2 and P-O1) (c). The thickness of lines shows the strength of the J_n coupling. AF and FM couplings and the absence of coupling are indicated by solid, dashed and dotted lines, respectively. The possible FM \rightarrow AF transitions are shown by strokes in dashed lines.

ferromagnetic. There is a weak competition between one AF $J5$ coupling and two weak FM $J10$ and $J11$ couplings, which form a distorted triangle $J5J10J11$, since these couplings are not equal in strength ($J5 = -2.4(-5.1 \text{ and } -5.3)$ $J10 = -7.1(-9.1 \text{ and } -9.4)$ $J11$ in $Tb(Bi-RT \text{ and } Bi-LT)$ systems). Besides, the FM $J10$ and $J11$ couplings compete with the AF inter-dimer couplings $J8$ and $J9$ in the distorted triangles $J8J10J11$ and $J9J10J11$.

Comparatively strong AF J_{a1} and J_{b1} couplings exist between the $Mn1$ ions, which are located through the elementary unit parameters along the a and b axes, while along the c axis the J_{c1} ($J_{c1} \equiv J_2$) coupling is ferromagnetic, but could undergo the phase transition FM \rightarrow AF, as shown above. Similar couplings between the $Mn2$ ions are significantly weaker and do not always have the same sign: the J_{b2} and J_{c2} couplings are antiferromagnetic, and the J_{c2} coupling could undergo the phase transition AF \rightarrow FM (intermediate O1 and O4 ions are located in the critical position ‘b’), while the J_{a2} coupling is ferromagnetic.

One should mention that the parameters of magnetic coupling, which we calculated in accordance with the structural data of the Wang polar model [7, 8] (table 1), are similar to those of the frustrated paraelectric phase $TbMn_2O_5$ (table 3).

Thus, the paraelectric phases of $TbMn_2O_5$ and $BiMn_2O_5$ are frustrated antiferromagnetics. In linear chains along the c axis, the nearest AF $J1$ and $J2$ couplings compete with the next-to-nearest-neighbor (J_n) couplings. In addition, the $J1$ and $J2$ couplings compete with all strong AF $J3$, $J4$, $J6$ and $J7$ couplings between linear chains and dimers. However, the AF intra-chain $J1$ and $J2$ couplings are unstable and could be eliminated or transformed into the FM state, resulting in magnetic ordering, even at slight displacement of intermediate O2, O3 and O4 ions from the bond line $-Mn1-Mn1-$. Further, we will consider the relation of magnetic ordering to the emerging of electric polarization.

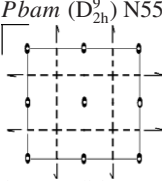
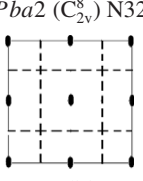
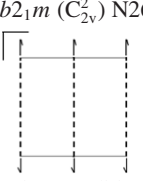
3.2. Necessary conditions for emerging ferroelectricity in $TbMn_2O_5$ and $BiMn_2O_5$

The crystal structure of $Tb(Bi)Mn_2O_5$ is not typical for ferroelectrics, since in the paraelectric phase it contains atomic groups in the form of $Mn1^{4+}O_6$ octahedra and $Mn2^{3+}O_5$ pyramids having constant dipole moments; however, coupling in these groups is of substantially ionic character. The dipoles in these groups are oriented in different directions. The gravity centers of positive and negative centers in $Mn^{4+}O_6$ distorted octahedra and $Mn^{3+}O_5$ pyramids do not coincide (tables 1 and 2; figures 2(a) and (b)). In $Mn1O_6$ octahedra the $Mn1$ is displaced (by ~ 0.07 ($\sim 0.06 \text{ \AA}$) in $Tb(Bi)$ systems) along the c axis from the octahedron center to the O3–O3 edge, which makes the $Mn1-O3$ distances in the octahedron equatorial plane shorter (by $\sim 0.1 \text{ \AA}$) than the $Mn1-O2$ distances. The distances to the O4 ions in octahedron axial vertices are approximately equal to the average value of the long $Mn1-O2$ and short $Mn-O3$ bond lengths. The dipole moments of octahedra in the chain are oriented antiparallel and directed along the c axis.

In dimers the $Mn2$ are displaced from the $Mn^{3+}O_5$ pyramid centers to the O4–O4 edges in $TbMn_2O_5$ and in the opposite direction to the common O1–O1 edge in $BiMn_2O_5$. As a result, the $Mn2-O4$ bond lengths in $TbMn_2O_5$ are shorter (by 0.04 \AA) than the $Mn2-O1$ bond lengths while in $BiMn_2O_5$, in contrast, they are longer (by $0.03(0.02)$ in $Bi-RT(Bi-LT)$ systems). The dipole moments of pyramids in dimers are oriented antiparallel and directed along the b axis. However, the direction of dipoles in $TbMn_2O_5$ is changed by 180° relative to that in $BiMn_2O_5$.

For emerging spontaneous polarization in RMn_2O_5 it is necessary to perform ordering of dipoles of the $Mn^{4+}O_6$ octahedra and $Mn^{3+}O_5$ pyramids in the same direction or eliminate the dipole moment in one of the groups while ordering dipoles in another group. Changing the orientation of dipole moments of octahedra and pyramids is possible due to displacement of specific ions, because couplings in these dipole groups are not ‘rigid’. It is not the rigidity of coordination polyhedra of Mn^{3+} and Mn^{4+} (see section 1) that

Table 5. Comparison of the positions in the space group *Pbam* and its subgroups *Pba2* and *Pb2₁m*.

<i>Pbam</i> (D_{2h}^9) N55		<i>Pba2</i> (C_2^8) N32		<i>Pb2₁m</i> (C_{2v}^2) N26	
					
Reflection conditions $0kl: k = 2n; h0l: h = 2n;$ $h00: h = 2n; 0k0: k = 2n$		Reflection conditions $0kl: k = 2n; h0l: h = 2n;$ $h00: h = 2n; 0k0: k = 2n$		Reflection conditions $0kl: k = 2n; 0k0:$ $k = 2n$	
Position Atom	Coordinates	Position Atom	Coordinates	Position Atom	Coordinates
8 <i>i</i>	$x, y, z; -x, -y, z$	4 <i>c</i> :	$x, y, z;$	4 <i>c</i> :	x, y, z
O4	$-x + 1/2, y + 1/2, z;$ $x + 1/2, -y + 1/2, z$ $-x, -y, -z; x, y, -z$ $x + 1/2, -y + 1/2, -z;$ $-x + 1/2, y + 1/2, -z$	O4 (<i>x, y, z</i>)	$-x, -y, z;$	O4 ($x + 1/4, y, z$);	$-x, y + 1/2, z$
4 <i>h</i>	$x, y, 1/2;$	O4' ($-x,$	$-x + 1/2,$	O4'	$x, y, -z$
Mn2, O3	$-x, -y, 1/2$ $-x + 1/2, y + 1/2, 1/2;$ $x + 1/2, -y + 1/2, 1/2$	$-y, -z)$	$y + 1/2, z;$	$(-x + 1/4, -y, -z)$	$-x, y + 1/2, -z$
4 <i>g</i>	$x, y, 0;$	4 <i>c</i> :	$x + 1/2,$	2 <i>b</i> :	$x, y, 1/2$
R, O2	$-x, -y, 0$ $-x + 1/2, y + 1/2, 0;$ $x + 1/2, -y + 1/2, 0$	Mn2, O3	$-y + 1/2, z$	Mn2, O3	$-x, y + 1/2, 1/2$
4 <i>f</i>	$0, 1/2, z; 1/2, 0, z;$	4 <i>c</i> :	$x, y, \sim 1/2;$	($x + 1/4, y, 1/2$);	
Mn1	$0, 1/2, -z; 1/2, 0, -z$	R, O2	$-x, -y, \sim 1/2;$	Mn2', O3'	$(-x + 1/4, -y, 1/2)$
4 <i>e</i>	$0, 0, z; 1/2, 1/2, z$	4 <i>c</i> :	$-x + 1/2,$	2 <i>a</i> :	$x, y, 0;$
O1	$0, 0, -z; 1/2, 1/2, -z$	Mn1	$y + 1/2, \sim 0;$	R, O2 ($x + 1/4, y, 0$)	$-x, y + 1/2, 0$
		Mn1' ($-z$)	$x + 1/2,$	R', O2'	$(-x + 1/4, -y, 0)$
			$-y + 1/2, \sim 0$	4 <i>c</i> :	x, y, z
				Mn1 ($\sim 1/4, \sim 1/2, z$)	$-x, y + 1/2, z$
					$x, y, -z$
					$-x, y + 1/2, -z$
					x, y, z
					$-x, y + 1/2, z$
					$x, y, -z$
					$-x, y + 1/2, -z$

allows changing the bond lengths in wide ranges. However, to attain the compound's stable state it is necessary to approximate the sum of bond valences to the cation ideal valence. The presence of common O3 and O4 ions for chains and dimers cause interrelation of any structural changes in these fragments.

The process of emerging electric polarization will be considered for two non-centrosymmetrical space groups *Pba2* and *Pb2₁m*, which comprise subgroups of the space group *Pbam* and belong to the *mm2* symmetry class. The atom positions for Tb(Bi)Mn₂O₅ in the space group *Pbam* and its subgroups *Pba2* and *Pb2₁m* are presented in table 5.

At first glance, the space group *Pba2* seems to be the most suitable for the ferroelectric transition, since it has the same reflection conditions with the centrosymmetrical space group *Pbam* and is indistinguishable from it in x-ray pictures. However, in this group the *c* axis serves as the polar axis while the magnetoelectric measurements show that spontaneous polarization occurs along the *b* direction. Nevertheless, it was of interest for us to find out why the *b*

direction had become more preferable than the *c* direction. In the *Pba2* space group the positions of Mn1(Mn⁴⁺), O1 and O4 ions are split into two kinds of sites.

The *b* axis serves as the polar axis in the non-centrosymmetrical space group *Pb2₁m*. Transition into this space group is concerned with the emerging of additional reflections. However, they were not found during the crystal studies by x-ray and neutron diffraction methods in the absence of external fields. In the space group *Pb2₁m* the positions of Mn2, O2, O3 and O4 ions are split into two kinds of sites. Besides, it is necessary to displace all atoms by 1/4 along the *x* axis relative to their values in the initial space group *Pbam*.

3.3. Magnetic ordering as the cause of structural instability of TbMn₂O₅ and BiMn₂O₅

We have shown above that, for the emerging of magnetic ordering in RMn₂O₅, it is sufficient to eliminate or transform the *J1* and *J2* couplings into the FM state. It is possible as a result of displacements of the O2 and O3 ions, which are

located in critical positions and make substantial contributions to the AF component of the above interactions, along the a axis from the line $-\text{Mn1}-\text{Mn1}-$. However, the displacements of the O2 and O3 ions in this direction are not polar; they just allow eliminating dipole moments in the Mn^{4+}O_6 octahedra chain that result in fulfilling only one of the conditions for the emerging of ferroelectricity in these compounds. Moreover, such displacements can be made in all three space groups under consideration, including the initial centrosymmetrical $Pb\bar{3}m$ group.

Unfortunately, we do not still have reliable data on the changes in positions of not only oxygen anions, but also of manganese cations under the effect of high magnetic fields. That is why to calculate the values of displacements of oxygen ions accompanying the emerging of the magnetically ordered state and ferroelectric polarization we used the elementary unit parameters and Mn ion coordinates obtained at a temperature 27 K for TbMn_2O_5 in [3, 4] and at 100 K for BiMn_2O_5 in [11]. The initial oxygen cations for oxygen atoms were taken for TbMn_2O_5 from [35] and for BiMn_2O_5 from [11].

By varying the x coordinates of O2 and O3 ions, it is easy to calculate, by using equation (4) and the ‘MagInter’ software, their values at which the distances $h(\text{O2})$ and $h(\text{O3})$ would increase (by $\sim 0.13\text{--}0.14$ Å) up to 1.40 Å while the $j(\text{O2})$ and $j(\text{O3})$ contributions, respectively, would decrease down to 0 (see section 3.1). According to the calculations, magnetic ordering is accompanied by an increase of the x coordinate of the O2 ions by 0.019(0.018) and of the O3 ions by 0.022(0.021) relative to the initial coordinates of these ions in the paraelectric phase of Tb(Bi) compounds. Besides, in TbMn_2O_5 we displaced the O4 ion along the c axis by 0.038 Å, thus increasing its z coordinate by just ~ 0.007 , in order to decrease the probability of emerging competition of J_1 and J_2 with J_3 and J_3' couplings. As a result of the performed displacements, the $d(\text{Mn1}-\text{O2})$ and $d(\text{Mn1}-\text{O3})$ bond lengths in the octahedron increased up to 2.013(2.047) Å and 1.968(1.968) Å, respectively, while the $d(\text{Mn2}-\text{O3})$ bond length in the pyramid, in contrast, decreased down to 1.868(1.935) Å in Tb(Bi) compounds. It resulted in partial equalization of the $d(\text{Mn1}-\text{O2})$ and $d(\text{Mn1}-\text{O3})$ lengths in Mn1O_6 octahedra. Another important effect of the displacements consists in equalization of the bond valences between the Mn1 and Mn2 atoms whose values became 3.42(3.29) and 3.56(3.32), respectively, while the initial values of bond valences for Mn1 and Mn2 equal to 4.01(3.86) and 3.18(3.11), respectively, were close to the ideal values.

Therefore, emerging of magnetic ordering is accompanied by the reduction of dipole moments of the Mn1 octahedra and charge disordering between the Mn1 and Mn2 positions.

Complete elimination of the Mn1O_6 octahedral dipoles accompanies the transition of the J_2 couplings to the FM state. The models of TbMn_2O_5 and BiMn_2O_5 compounds with the ordered magnetic structure and the absence of dipole moments in Mn1O_6 octahedra are marked as ‘M-DO’.

For M-DO models of Tb and Bi compounds the structural parameters, bond distances and bond valences of Mn1 and Mn2 ($V_{\text{Mn1}}, V_{\text{Mn2}}$) are presented in tables 1 and 2 while the parameters of magnetic coupling calculated in the

centrosymmetrical space group $Pb\bar{3}m$ are given in tables 3 and 4.

In such a transition the $d(\text{Mn1}-\text{O2})$ and $d(\text{Mn1}-\text{O3})$ bond lengths are equalized due to further displacement along the x axis (by $\sim 0.009(0.016)$) of only one O3 ion which increases (by 0.045(0.079) Å) the Mn1–O3 bond lengths up to 2.013(2.047) Å in Tb(Bi) systems. As a result, the Mn1 charge decreases down to 3.30(3.07) Å while the Mn2 charge, in contrast, increases up to 3.70(3.54) Å. In fact, there proceeds an exchange of bond valence values between the Mn1 and Mn2 positions, i.e. a new charge ordering emerges that is the reverse of the initial one. As a result, the crystal structure becomes unstable, since for Jahn–Teller Mn^{3+} ions the surrounding coordination in the form of a flattened-out octahedron is not advantageous [39] while for the Mn^{4+} ions the surrounding coordination in the form of a square pyramid is not characteristic.

According to the calculations, all the respective magnetic couplings at magnetic ordering accompanied by a decrease as complete elimination of octahedral dipole moments are virtually identical, except for the J_2 couplings. In the first case the J_2 couplings are eliminated while in the second case they are comparatively strong FM couplings. In the chain along the c axis the nearest-neighbor J_1 and J_2 and the next-nearest-neighbor J_2, J_3, J_3' and J_4 couplings do not compete with each other, since they become ferromagnetic. The parameters of strong AF intra-dimer J_5 coupling, J_3, J_6 (along the b axis) and J_4, J_7 (along the a axis) couplings in the ab plane did not virtually change relative to the parameters in the frustrated phase. Only two weaker AF couplings between the Mn2 ions— J_8 (in the ab plane) and J_{c2} (located through the parameter c)—undergo the phase transition AF \rightarrow FM with increasing interaction strength. As a result, in the magnetically ordered structure the competition in the $J_2J_3J_3', J_2J_4J_4', J_1J_3J_6, J_1J_4J_7, J_8J_3J_3', J_8J_6J_6$ and $J_8J_10J_11$ triangles disappears; however, a weak competition is preserved in the $J_9J_4J_4', J_9J_7J_7'$ and $J_5J_10J_11$ triangles, where the couplings are not equal in strength, and in the $J_9J_10J_11$ triangle, where all three interactions are weak (figure 3).

3.4. Ferroelectric transition as the way of removing structural instability

It is possible to return a stable state to the magnetically ordered structure of Tb(Bi) Mn_2O_5 only by approximation of the bond valences of Mn1 and Mn2 to the initial values of ~ 4 and ~ 3 , respectively. In other words, it is necessary to make the charge exchange or redistribute charges between Mn1 and Mn2. Under the magnetic ordering condition and elimination of the octahedral dipoles, when the O2, O3 and Mn1 ions are fixed, it is possible exclusively by displacements of the O4, O1 and Mn2 ions along the b axis. Transition from the centrosymmetrical $Pb\bar{3}m$ to the non-centrosymmetrical space group $Pb2_1m$ allows, simultaneous with increasing the bond valence of Mn1 and decreasing the bond valence of Mn2, the emerging of spontaneous electrical polarization due to displacements of the Mn2, O1 and O4 ions along the b axis,

which are polar in this group (figure 2(c)). Transition to the space group $Pba2$ does not produce the required result, since polar displacements in this group comprise those along the c axis. However, they cannot effectively change the Mn1–O4 and Mn2–O4 bond lengths and, respectively, the bond valences of Mn1 and Mn2 and stabilize the structure.

In the displacement-type ferroelectrics polarization is, as a rule, related to the cation displacement from the center of its surrounding oxygen octahedron, while the positions of all other atoms remain unchangeable, and has the same direction as the displacement. Transition of the non-polar modification of the M-DO model to the polar modification is complicated by two circumstances. First, the restructuring must be accompanied by specific changes in bond valences of Mn1 and Mn2 (see section 3.3). Second, the Mn2 cations in the non-polar modification of the M-DO model are already located not in the center of a square pyramid. That is why to separate the gravity centers of positive and negative charges in the M-DO-model structure the displacements of only cations are not sufficient.

We suggest two polar models P-Mn2 and P-O1 within the frames of the space group $Pb2_1m$. In both models the polarization effect was achieved by reducing the lengths of the Mn2–O1, Mn2'–O4' and Mn1–O4 bonds oriented along the b axis and increasing the lengths of the Mn2'–O1, Mn2–O4 and Mn1–O4' bonds oriented along the same axis, but antiparallel to the shortened bonds (tables 1 and 2; figure 2(c)). During the development of polar models the ion displacements were performed relative to their positions in the M-DO-model.

The polar P-Mn2 model for Tb(Bi) systems is formed by displacements of both Mn2 and Mn2' cations (by $\sim 0.02(0.05)$ Å) at equal distances along the b axis in the same direction and the O4 anion displacements (by $\sim 0.13(0.18)$ Å) and O4' (by $\sim 0.11(0.12)$ Å) along the b axis as well, but in opposite directions and at different distances. As a result of the performed displacements, the bond valence of Mn1 increased by 0.45(0.54) and the bond valences of Mn2 and Mn2' decreased by 0.30(0.40) in Tb(Bi) systems and noticeably approached the ideal values. The polar model P-O1 was developed only due to the oxygen anion displacements. We just substituted the Mn2 and Mn2' displacements in the P-Mn2 model by those of the O1 anions of the same value, but in the opposite direction, and decreased the O4' ion displacements (down to $\sim 0.09(0.07)$ Å in Tb(Bi) systems). This resulted in the values of the Mn1, Mn2 and Mn2' bond valences approximately the same as in the P-Mn2 model (tables 1, 2).

Nevertheless, in both P-Mn2 and P-O1 models we achieved the effect of cation displacements along the b axis in one direction: the Mn1 ion approaches the O4 octahedron vertex, the Mn2 ion the O1–O1 pyramid edge and the Mn2' ion the O4'–O4' pyramid edge (figure 2(c)). If one changes the direction of ion displacements along the b axis to the opposite, polarization will be changed by 180° : the Mn1 ion approaches the O4' vertex, the Mn2 ion the O4–O4 edge and the Mn2' ion the O1–O1 edge. One should mention that in these models we deliberately increased the O4 ion displacement value more than necessary, as compared to that of the O4' ion, in order to demonstrate the possibility of participation of both Mn1 and Mn2 ions in polarization.

A principal difference between these models consists in the fact that the displacement of the Mn2 and Mn2' ions in the same direction along the b axis in the P-Mn2 model results, in addition, in opposite values of the change of the Mn2–O3 and Mn2–O3' distances. This very fact could be the cause of the disappearing symmetry center in the crystal structures of TbMn₂O₅ and BiMn₂O₅.

The electric polarization is induced and maintained by magnetic ordering which emerges and exists under an external magnetic field. According to the calculations, the parameters of magnetic couplings in polar P-Mn2 and P-O1 models are virtually identical to the respective values in the M-DO model with ordered magnetic structure (tables 3 and 4).

4. Conclusions

We have shown the role of crystal structure in the emerging magnetic ordering and electric polarization in TbMn₂O₅ and BiMn₂O₅. According to the calculations, the sign and strength of magnetic couplings found on the basis of structural data show that the paraelectric phase of TbMn₂O₅ and BiMn₂O₅ is a frustrated antiferromagnetic. In linear chains of Mn1⁴⁺ along the c axis the nearest AF $J1$ and $J2$ couplings compete with the next-to-nearest-neighbor J_n couplings. In addition, the $J1$ and $J2$ couplings compete with all strong AF $J3$, $J4$, $J6$ and $J7$ couplings between linear chains of Mn1⁴⁺ and dimers of Mn2³⁺. The elimination or transformation of the $J1$ and $J2$ couplings into the FM state is sufficient for the emerging magnetic ordering in Tb(Bi)Mn₂O₅. The latter is possible through slight displacements of intermediate ions (O2 and O3 ions from the line –Mn1–Mn1– along the a axis and O4 ions along the c axis), which are in critical positions. However, these displacements accompanying magnetic ordering are not polar; depending on the value, they just induce equalizing (charge disordering) or value exchange (new charge ordering) of the bond valences between the Mn1 and Mn2 ions, thus creating instability of the crystal structure. To approximate again the bond valence of Mn1 and Mn2 to the initial value under the magnetic ordering conditions is possible only due to displacement of Mn2 (or O1) and O4 ions along the b axis that is the cause of the ferroelectric transition.

To sum it up, the fundamental cause of multiferroicity in the compounds under study is magnetic ordering of Tb(Bi)Mn₂O₅ under the effect of an external magnetic field accompanied by charge disordering that, in turn, induces the structural instability. In the second stage, only the charge ordering transition takes place, thus inducing ferroelectricity and restoring the structural stable state while preserving magnetic ordering. Our studies are in agreement with the recent work by Brink and Khomskii [40], where the generic mechanisms by which charge ordering can induce ferroelectricity in magnetic systems are presented. To obtain direct experimental evidence of the presence of structural changes accompanying the spontaneous polarization, one should perform diffraction studies of induced multiferroics exclusively under high magnetic fields.

References

- [1] Hur N, Park S, Sharma P A, Ahn J S, Guha S and Cheong S-W 2004 *Nature* **429** 392
- [2] Hur N, Park S, Sharma P A, Guha S and Cheong S-W 2004 *Phys. Rev. Lett.* **93** 107207
- [3] Chapon L C, Blake G R, Gutmann M J, Park S, Hur N, Radaelli P G and Cheong S-W 2004 *Phys. Rev. Lett.* **93** 177402
- [4] Blake G P, Chapon L C, Radaelli P G, Park S, Hur N, Cheong S-W and Rodriguez-Carvajal J 2005 *Phys. Rev. B* **71** 214402
- [5] Chapon L C, Radaelli P G, Blake G R, Park S and Cheong S-W 2006 *Phys. Rev. Lett.* **96** 097601
- [6] Kagomiya I, Matsumoto S, Kohn K, Fukuda Y, Shoubu T, Kimura H, Noda Y and Ikeda N 2003 *Ferroelectrics* **286** 167
- [7] Wang C, Guo G-C and He L 2007 *Phys. Rev. Lett.* **99** 177202
- [8] Wang C, Guo G-C and He L 2007 arXiv:0711.2539 [cond-mat]
- [9] Cheong S-W and Mostovoy M 2007 *Nature* **6** 13
- [10] Golovenchits E and Sanina V 2004 *J. Phys.: Condens. Matter* **16** 4325
- [11] Granado E, Eleotério M S, García-Flores A F, Souza J A, Golovenchits E I and Sanina V A 2008 *Phys. Rev. B* **77** 134101
- [12] Dela Cruz C R, Yen F, Lorenz B, Gospodinov M M, Chu C W, Ratcliff W, Lynn J W, Park S and Cheong S-W 2006 *Phys. Rev. B* **73** 100406
- [13] Narumi Y, Kindo K, Katsumata K, Kawauchi M, Broennimann Ch, Staub U, Toyokawa H, Tanaka Y, Kikkawa A, Yamamoto T, Hagiwara M, Ishikawa T and Kitamura H J 2006 *Synchrotron Radiat.* **13** 271
- [14] Matsuda Y H, Ueda Y, Nojiri H, Takahashi T, Inami T, Ohwada K, Murakami Y and Arima T 2004 *Physica B* **346/347** 519
- [15] Frings P, Vanacken J, Detlefs C, Duc F, Lorenzo J E, Nardone M, Billette J, Zitouni A, Bras W and Rikken G 2006 *Rev. Sci. Instrum.* **77** 063903
- [16] Detlefs C, Duc F, Kaze Z A, Vanacken J, Frings P, Bras W, Lorenzo J E, Canfield P C and Rikken G 2008 *Phys. Rev. Lett.* **100** 056405
- [17] Vanacken J, Frings P, Detlefs C, Duc F, Lorenzo J E, Nardone M, Billette J, Zitouni A, Bras W and Rikken G 2006 *J. Phys.: Conf. Ser.* **51** 475
- [18] Alonso J A, Casais M T, Martínez-Lopez M J and Rasines I J 1997 *Solid State Chem.* **129** 105
- [19] Kagomiya I, Kohn K and Uchiyama T 2002 *Ferroelectrics* **280** 131
- [20] Popov G, Greenblatt M and McCarroll W H 2000 *Mater. Res. Bull.* **35** 1661
- [21] Zouari S, Ranno L, Cheikh-Rouhou A, Isnard O, Pernet M, Wolfers P and Strobel P 2003 *J. Alloys Compounds* **353** 5
- [22] Jansen M, Chang F M and Hoppe R Z 1982 *Anorg. Allg. Chem.* **490** 101
- [23] Brachtel G and Hoppe R Z 1980 *Anorg. Allg. Chem.* **468** 130
- [24] Kaiser J W and Jeitschko P D W 2000 *Z. Kristallogr.* **215** 313
- [25] Teichert A and Mueller-Buschbaum H 1991 *Z. Anorg. Allg. Chem.* **598** 319
- [26] Wakiya K, Sato H, Miyazaki A, Enoki T, Isobe M and Ueda Y 2001 *J. Alloys Compounds* **317** 115
- [27] Chang F M and Jansen M Z 1985 *Anorg. Allg. Chem.* **531** 177
- [28] Zubkov V G, Tyutyunnik A P, Berger I F, Voronin V I, Bazuev G V, Moore C A and Battle P D 2002 *J. Solid State Chem.* **167** 453
- [29] Volkova L M and Polyshchuk S A 2005 *J. Supercond.* **18** 583 (arXiv:cond-mat/0504599v3)
- [30] Kramers H A 1934 *Physica* **1** 182
- [31] Goodenough J B 1955 *Phys. Rev.* **100** 564
- Goodenough J B 1963 *Magnetism and the Chemical Bond* (New York: Wiley)
- Kanamori J 1959 *J. Phys. Chem. Solids* **10** 87
- Anderson P W 1963 *Solid State Physics* vol 14, ed F Seitz and D Turnbull (New York: Academic) pp 99–214
- [32] Vonsovsky S V 1971 *Magnetism* (Moscow: Nauka)
- [33] Sheldrick G M 2008 *Acta Crystallogr. A* **64** 112
- [34] Shannon R D 1976 *Acta Crystallogr. A* **32** 751
- [35] Alonso J A, Casais M T, Martínez-Lopez M J, Martínez J L and Fernandez-Diaz M T 1997 *J. Phys.: Condens. Matter* **9** 8515
- [36] Munoz A, Alonso J A, Casais M T, Martínez-Lope M J, Martínez J L and Fernandez-Diaz M T 2002 *Phys. Rev. B* **65** 144423
- [37] Brese N B and Keefe M O 1991 *Acta Crystallogr. B* **47** 192
- [38] Smith R W and Keszler D A 1991 *J. Solid State Chem.* **93** 430
- [39] Kugel K I and Khomskii D I 1982 *Usp. Fiz. Nauk* **136** 621
- [40] Van den Brink J and Khomskii D I 2008 Preprint <http://de.arxiv.org/abs/0803.2964v3>